TOPOLOGY OPTIMIZATION FOR LIGHTWEIGHTING ANISOTROPIC ADDITIVELY MANUFACTURED PARTS UNDER THERMOMECHANICAL LOADING

Jack Ramsey, Dr. Douglas Smith
Baylor University

Abstract

Topology optimization has emerged as an effective design approach that can optimize the performance of lightweight automotive parts having complex geometries that is ideally suited for additive manufacturing. However, most additively manufactured structures have anisotropic material properties, especially those composed of fiber-filled polymers. In addition, residual thermal stresses arise from nonisothermal cooling processes during manufacturing which has yet to be incorporated into topology optimization. This paper presents a new topology optimization-based approach that incorporates both material anisotropy and weakly coupled thermomechanical loading into the design computations. In our approach, design derivatives are evaluated using the adjoint variable method specifically for the weakly coupled thermomechanical system. An optimality criterion-based update scheme minimizes the compliance or strain energy within the design space over material density and anisotropic orientation. The coupled thermomechanical analysis and material direction optimization reflects the anisotropic Young's modulus and thermal stresses present in large-scale polymer deposition. Resultant structures show how thermal loading influences the optimal topology.

Introduction

Motivation

Additive manufacturing has opened tremendous design freedom by allowing for added design complexity at little or no additional cost. Early additively manufactured parts were used primarily for prototypes due to part weakness and inaccuracy, but recent developments in reliability and strength improvement allow additive manufactured parts to perform well as end-use parts. These parts can be extremely useful in lightweighting applications due to the ease of producing parts having complex geometric features.

However, traditional part design methods do not take advantage of the design freedom present in additive manufacturing. New design methods must be developed to fully optimize the performance of these parts. Topology optimization methods can be modified to do that by modeling the unique fabrication methods common in the additive manufacturing process.

The topology optimization algorithm used here modifies the optimality criterion method to optimize the design of a two-dimensional anisotropic part with spatially varying material properties under steady state weakly coupled thermoelastic loading. The material anisotropy and thermally induced stresses are included to simulate the thermal aspects of a typical additive manufacturing process. The constrained minimization problem is solved with an optimality criteria-based method over material density and orientation to minimize the compliance or strain energy of a structure. The design sensitivities are derived for both compliance and strain energy, and the method is implemented through a custom finite element program in Matlab. The optimized topologies can be obtained and compared, and proof-of-concept parts can be printed to demonstrate the viability of the method.

Topology Optimization

Topology optimization seeks to determine the geometry or material layout of a part that achieves the best performance. Bendsoe and Kikuchi first introduced topology optimization in 1988 [1] to minimize the compliance of a structural part via the homogenization method. Over the next thirty years, several other methods have been developed, such as the optimality criterion method [2], the level-set method [3], and the method of moving asymptotes [4]. These have been applied to the basic structural compliance problem and have also been used in structures with multiple loading conditions, to optimize the performance of heat sinks, optimize the fundamental frequency of vibration, and create compliant mechanisms. Topology optimization has been used to develop parts with multiphase materials, anisotropic material properties, and piezoelectric properties. Bendsoe and Sigmund give numerous examples of the application of topology optimization [5].

Additively manufactured materials are often highly anisotropic, which has been modeled in topology optimization for the structural compliance problem. The original work by Bensoe and Kikuchi [1], and much of the work to follow, focused on computing optimal structures using anisotropic materials. More recently, Hoglund [6] developed a method that optimizes the compliance of anisotropic parts which focused on its application in additive manufacturing. His work was extended to three-dimensional parts by Jiang [7], [8] for use in big-area additive manufacturing. They used a general Matlab optimizer instead of a pre-existing optimization method (as in [2]), which demonstrated the viability of the technique. Drs. Luo and Gea utilized a similar method [9].

Another distinctive feature of the additive manufacturing process is the thermal response during processing as most AM methods require significant localized heating followed by an overall cooling of the part. Nonisothermal aspects have only been implemented partially into topology optimization, appearing as an isothermal weakly coupled thermomechanical system in the literature. To the best of the author's knowledge, no design-dependent temperature problem has been coupled to a mechanical analysis. Deaton [10] optimized the performance of parts under constant temperature increase for aircraft fuselages. It was determined by Pedersen and Pedersen [11] that optimizing compliance in isothermal weakly coupled thermomechanical systems does not always maximize strength, and they proposed alternative optimization functions. Zhang, et al, [12] compared optimizing compliance and strain energy, and showed that optimizing strain energy may yield a lower maximum stress. This was also done with the level-set method by Neiford, et al, who also optimized the maximum displacement [13].

Overall, parameters that enter the additive manufacturing process have only been partially explored in topology optimization. Anisotropic materials have only been considered with pure mechanical loading, and the methods are robust but can be computationally intensive. Weakly coupled thermomechanical systems with design-dependent loading have been considered only for given temperature fields. The goal of this paper is to extend this work to design-dependent temperature fields which introduces significant complexity.

Challenges in Additive Manufacturing

The structures designed by topology optimization are frequently complex enough that the structure cannot be manufactured with traditional methods. The ongoing development of additive manufacturing from a prototyping technique to a robust manufacturing method has brought topology optimization from a mostly theoretical design strategy to a practical tool for creating extremely strong, lightweight parts. The printing process can be controlled precisely enough to yield accurate parts, but the effects from the printing process, specifically the thermal aspects, still affect part performance.

In most polymer composite additive manufacturing systems, such as fused-filament fabrication or large-scale polymer deposition extrusion, the polymer melts as it is extruded and deposited on material below. During this process the polymer strands are aligned partially in the direction of deposition, and weaker bonding between extruded beads exacerbates this anisotropy in the print direction. Different print patterns seek to alternate the bead direction in subsequent layers to approximate an isotropic material, but do not fully take advantage of the increased strength in the print direction.

In polymer deposition additive manufacturing, the printed material is made stronger and stiffer by adding continuous or short chopped glass or carbon fibers to the polymer. In this process, fibers tend to align with the bead while the molten polymer is extruded, so the strength and stiffness increase most in the print direction. Parts can have an elastic modulus twice as high in the direction of print [14] and optimizing the part geometry and print direction with respect to this can significantly improve part performance.

Carbon and glass fibers have a lower coefficient of thermal expansion than the surrounding polymer, which can reduce the thermal stress and part warpage that arises as the polymer composite part cools. Each subsequent layer cools partially before the next is added, creating complicated deformation and stress patterns perpendicular to the build plane. Even when no deformations are visible, the part can have internal thermal stresses that alter its behavior under loading. Depending on the loading condition, these can be beneficial or counterproductive, and must be considered.

Obtaining effective geometric designs for parts produced with the additive manufacturing process present challenges that topology optimization methods are beginning to investigate. The material location and orientation must be simultaneously considered and optimized to reflect the anisotropic extrusion process and fiber reinforcement. Including the weakly coupled thermomechanical analysis to capture manufacturing related thermal stresses as the part cools such as is done in this paper is also needed. The algorithm presented here unites techniques for the anisotropy and thermal stresses for one cohesive method that captures both the printing process and the use of the final part.

Methods

Definition of Design Problem

The topology optimization method developed in this work considers a single part. A two-dimensional design domain is defined and discretized into equal square linear finite elements. The constituent equations for linear steady-state thermal conduction and linear elasticity are defined across the entire part domain which is discretized into finite elements in the usual manner. The steady thermal conduction analysis is employed to model nonisothermal aspects of the cooling process that occurs during the manufacturing of the part. However, it is understood that our steady-state thermal analysis does not fully reflect the complexity of the additive manufacturing process, but instead provides a significant first step in including both thermal and mechanical loading in topology optimization. The steady thermal analysis is weakly coupled with the mechanical analysis via thermal stresses, and the mechanical analysis models the part's performance in use.

In our approach, each 2-dimensional finite element has two design variables, the density x_i and the element orientation θ_i. Simple bounds are placed on element density variables restricting their range to be between 0 and 1. The density variable x_i defines the amount of material in the i-th element. The element orientation variable θ_i represents the direction of anisotropic material orientation which is defined in the AM process by the material deposition direction. The finite

element analysis includes an elemental thermal stiffness matrix K_{Th_i} which may be written in terms of the element design variables as

$$K_{Th_i} = x_i^p \int_{\Omega_i} B_{Th}^T R^T(\theta_i) D_{Th} R(\theta_i) B_{Th} d\Omega_i \tag{1}$$

where the subscript Th denotes the thermal stiffness matrix, p is a density penalty parameter used in the optimality criterion method described below, B_{Th} is the temperature gradient matrix, and D_{th} is the anisotropic thermal elasticity matrix. Similarly, the mechanical elemental stiffness matrix K_{M_i} is [6]

$$K_{M_i} = x_i^p \int_{\Omega_i} B_M^T R^T(\theta_i) D_M R(\theta_i) B_M d\Omega_i \tag{2}$$

where the subscript M denotes the mechanical stiffness matrix, p is the same penalty parameter used above, B_M is the displacement gradient matrix, and D_M is the anisotropic elasticity matrix, which can be written in terms of the anisotropic Young's Moduli and Poisson's ratios as [6]

$$D_M = \begin{bmatrix} \frac{E_x}{1-\nu_{xy}\nu_{yx}} & \frac{\nu_{xy}E_y}{1-\nu_{xy}\nu_{yx}} & 0 \\ \frac{\nu_{xy}E_y}{1-\nu_{xy}\nu_{yx}} & \frac{E_y}{1-\nu_{xy}\nu_{yx}} & 0 \\ 0 & 0 & G_{xy} \end{bmatrix} \tag{3}$$

Also, note that the standard rotation tensor can be written in terms of the element material angle θ_i as [6]

$$R(\theta_i) = \begin{bmatrix} cos^2(\theta_i) & sin^2(\theta_i) & -2 * sin(\theta_i) * cos(\theta_i) \\ sin^2(\theta_i) & cos^2(\theta_i) & 2 * sin(\theta_i) * cos(\theta_i) \\ sin(\theta_i) * cos(\theta_i) & -sin(\theta_i) * cos(\theta_i) & cos^2(\theta_i) - sin^2(\theta_i) \end{bmatrix} \tag{4}$$

In our algorithm we first perform the thermal analysis to obtain nodal temperatures which are used to compute thermal loads within each element. These thermal loads then serve as inputs to the mechanical analysis, weakly coupling the thermal problem to the linear elastic problem where the thermal load within the i-th element is evaluated from [15]

$$F_{TF_i} = x_i^p \int_{\Omega_i} B_M^T D_M R^T(\theta_i) \begin{Bmatrix} \alpha_x \\ \alpha_y \\ 0 \end{Bmatrix} R(\theta_i) N^T T_i d\Omega_i \tag{5}$$

where T_i are the nodal temperatures for the i-th element and N is the element shape function vector. In our examples, all elements are identically sized and square linear elements yielding identical shape functions across all elements. The coefficients of thermal expansion coefficients α_x and α_y are assumed to be different in each of the two coordinate directions due to the anisotropy of the printed structure.

The penalty method used here uses the penalty parameter p in Equations 1,2 and 5 to force the x_i to either 0 or 1 during the optimization similar to that defined in the solid isotropic material with penalization (SIMP) method, though other penalization methods can be used [8].

Globally, the finite element equations satisfy thermal equilibrium $K_{Th}T = F_{Th}$ and mechanical

equilibrium $KU = F$. Here, K_{Th} is the global thermal stiffness matrix and K is the global mechanical stiffness matrix, T is the global temperature vector and U is the displacement vector, and F_{Th} is the thermal flux vector and F is the mechanical load vector. The displacements due only to the thermal stresses U_{TF} can also be determined by $KU_{TF} = F_{TF}$.

Optimization Problem Statement

As stated above, the design variables are the element densities x_i and the element orientations θ_i. The topology optimization method seeks to minimize the objective function f written as a function of the design variables subject to a volume constraint which is stated mathematically as

$$minimize\ f(\overline{\boldsymbol{x}}, \overline{\boldsymbol{\theta}}) \tag{6}$$

$$subject\ to\ \frac{\sum x_i}{N_{el}} \leq V_f$$

where $\overline{\boldsymbol{x}}$ and $\overline{\boldsymbol{\theta}}$ are vectors of the element density and orientation design variables, respectively. The volume constraint is a function of element densities and limits the amount of material used to construct the part which is written in terms of the volume fraction V_f defined between 0 and 1. The part volume fraction V_f represents the fraction of the design space that can be filled with material. Note that N_{el} is the number of elements in the finite element discretization.

Two separate optimization functions are considered in this work. Compliance C, the inverse of stiffness, is classically considered as the objective function for topology optimization. It is defined in terms of the finite element displacement and applied force vectors, which may be written as a function of the design variables as

$$C(\overline{\boldsymbol{x}}, \overline{\boldsymbol{\theta}}) = U(\overline{\boldsymbol{x}}, \overline{\boldsymbol{\theta}})^T F(\overline{\boldsymbol{x}}, \overline{\boldsymbol{\theta}}) \tag{7}$$

where we assume that the applied force F is a sum of the design-dependent thermal stresses and the design-independent applied mechanical forces. Strain energy is considered as an alternate objective function, as recent work suggests minimizing strain energy generates parts with lower maximum Von Mises stresses [12]. The strain energy S is defined as

$$S(\overline{\boldsymbol{x}}, \overline{\boldsymbol{\theta}}) = \frac{1}{2} U(\overline{\boldsymbol{x}}, \overline{\boldsymbol{\theta}})^T F(\overline{\boldsymbol{x}}, \overline{\boldsymbol{\theta}}) - U(\overline{\boldsymbol{x}}, \overline{\boldsymbol{\theta}})^T F_{Th}(\overline{\boldsymbol{x}}, \overline{\boldsymbol{\theta}}) + \frac{1}{2} U_{Th}^T(\overline{\boldsymbol{x}}, \overline{\boldsymbol{\theta}}) F_{Th}(\overline{\boldsymbol{x}}, \overline{\boldsymbol{\theta}}) \tag{8}$$

where we note that the thermal load $F_{Th}(\overline{\boldsymbol{x}}, \overline{\boldsymbol{\theta}})$ is design dependent. Simple bounds are imposed on the design variables where densities are constrained to be between x_{min} and 1, where $x_{min} \ll 1$ is nonzero to prevent singularities from arising. In this work x_{min} is set to 0.001. The element orientations are bounded to remain between 0 and π, though they are considered via modular arithmetic and thus no hard boundary need be enforced.

It is desired that each element density approach either 1 or x_{min} as the algorithm progresses, because this ensures that material remaining in the design domain is best utilized. To this end, the penalty parameter p penalizes terms within the stiffness matrix, and similarly the thermal stress equation accomplishes this by artificially weakening elements with fractional density. The parameter p is traditionally set to 3, but is a tuneable parameter [2].

Optimality Criterion Update Scheme

The design formulation presented above may be solved with various optimization algorithms

defined to update the design variable values in an iterative manner. While our work uses an optimality criterion-based update method, other commonly used methods like the globally convergent method of moving asymptotes [4] utilize the same structure. Our optimality criterion-based method follows that employed by Sigmund [2] which updates the densities according to

$$x_i^{new} = \begin{cases} max(x_{min}, x_i - m), & if\ x_i B_i^{\eta} \leq max(x_{min}, x_i - m) \\ min(1, x_i + m), & if\ x_i B_i^{\eta} \geq min(1, x_i + m) \\ x_i B_i^{\eta}, & else \end{cases} \tag{9}$$

The move limit m is traditionally set to 0.2 for pure mechanical compliance optimization problems. The parameter B_i is defined in terms of the design sensitivity

$$B_i = \frac{\frac{-df}{dx_i}}{\lambda} \tag{10}$$

The objective function f is either compliance or strain energy, depending on the problem being solved. The Lagrange multiplier λ is constant for all densities and found with a bisection algorithm to preserve the volume fraction constraint as in Sigmund [2]. The damping constant $\eta = 0.5$ is used to stabilize the convergence but is a heuristic parameter that may be omitted from the formulation.

The element orientation design variables are updated independent of density since the optimal material angle can be considered to be a function of the local elemental stress field only. Each element is considered individually. The objective function value for the element is optimized given the element's nodal displacement vector U_i by treating the element orientation as a design variable. This is solved with a Newton-Raphson method to determine the optimal elemental orientation $\theta_{i_{min}}$. The orientation is then updated by moving it toward this optimal orientation, though the move limit L_i restricts the movement. Recall that the element orientations are considered modular with respect to π, so no bounds need be applied.

$$\theta_i^{new} = \begin{cases} \max(\theta_i - L_i, 0), & \theta_{i_{min}} < \theta_i - L_i \\ \theta_{i_{min}}, & abs(\theta_{i_{min}} - \theta_i) \leq L_i \\ \min(\theta_i + L_i, 2\pi), & \theta_{i_{min}} > \theta_i + L_i \end{cases} \tag{11}$$

where the move limit is dependent on the difference between the current angle and the ideal angle.

$$L_i = 0.1 * |\theta_i - \theta_{i_{min}}| \tag{12}$$

Design Sensitivities

The optimality criterion update scheme is gradient-based and thus requires the design sensitivities of the objective function. These are evaluated for the compliance objective function in Equation 7 using the adjoint variable method [16] for coupled systems to obtain

$$\frac{dC}{dx_i} = -px_i^{p-1}\, U_i^T K_i U_i + 2U_i^T \frac{\partial F_{th}}{\partial x_i} - 2px_i^{p-1} \left(\frac{\partial F_{th}}{\partial T} K_t^{-1}\right)_i K_{t_i} T_i \tag{13}$$

Note that the coupled effects of density and orientation on temperature, and then also the same on displacement, generate a more complex expression than the compliance sensitivity for a purely mechanical system [2]. The design sensitivity expression given above may be evaluated once the displacements and temperatures are computed and avoids the costly and unreliable finite difference calculations that are often used to obtain design derivatives. The design sensitivity of the strain energy objective function in Equation 8 using the adjoint variable method as

$$\frac{dS}{dx_i} = px_i^{p-1}\left(-\frac{1}{2}U_i^T K_i U_i + {U_{th_i}}^T K_i U - \frac{1}{2}U_{th_i}^T K_i U_{th_i}\right) \tag{14}$$

Note that the derivative expressions in Equations 13 and 14 are exact for the functions given in equations 7 and 8, respectively. The optimality criterion density update scheme in Equations 9 and 10 was first developed for compliance minimization under pure mechanical loading. In that case, the compliance sensitivities in Equation 13 are non-positive ensuring design convergence. However, in the presence of strong thermal loads, positive compliance sensitivities can exist which can prevent convergence, as the update scheme in Equations 9 and 10 may decrease element densities up to the move limit. To avoid the influence of positive sensitivities, we have found that the positive sensitivities can be mapped to zero.

$$\frac{dC}{dx_i}\Big|_{new} = \begin{cases} \dfrac{dC}{dx_i} & , \quad \dfrac{dC}{dx_i} < 0 \\ 0 & , \dfrac{dC}{dx_i} \geq 0 \end{cases} \tag{15}$$

Results

Optimal Design Computations

The algorithm described above was applied to a two-dimensional beam in three-point bending (the MBB beam), with a vertical force of $500\,N$ applied at top center. The half-symmetry finite element model appears in Figure 1. Previous work [17] showed that the structure of compliance-optimize and strain energy-optimized parts diverge as thermal loading increases, so a high thermal load was applied by fixing bottom edge at the ambient temperature and fixing the top edge at $10{,}000^0C$ above ambient temperature. This extremely high thermal loading is far in excess of most physical applications but more clearly demonstrates the differences in final topology. Both compliance and strain energy were optimized in separate optimizations for this loading case. The design domain was discretized into 400 by 200 square linear finite elements, and the centerline symmetry was used to halve the domain. A volume fraction of 0.5 was used, and the material's modulus of elasticity was 10 times higher in the direction of principle material orientation than perpendicular to it.

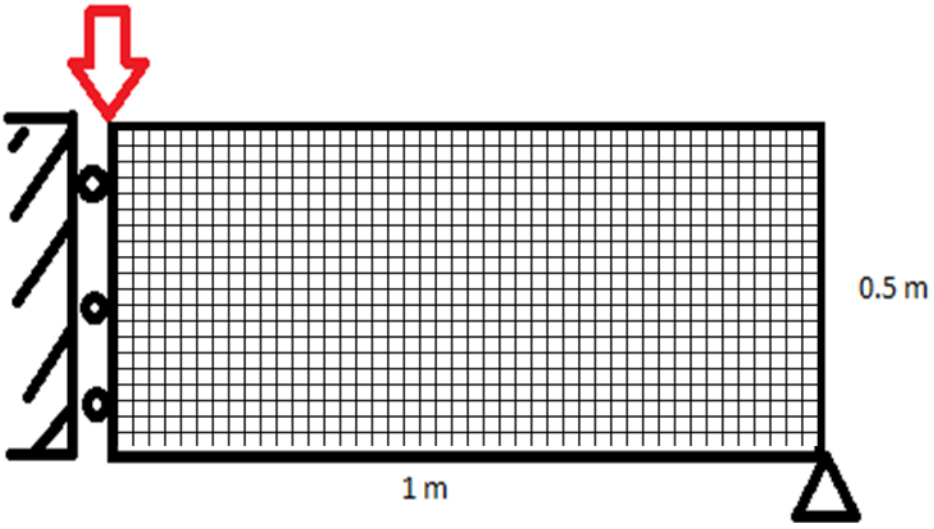

Figure 1: Design Domain

In the compliance optimization, the density move limit was set to 0.02 as the complexity of the design sensitivity prevents the first-order approximation from being accurate for larger ranges of density. Convergence was typically achieved in 100 iterations.

The strain energy optimization was performed for 4120 iterations with a density move limit of 0.02. The penalty was set to 4 instead of 3 to ensure convergence.

Final Topologies

The final topologies of the optimization are displayed below. Note that the color contours represent the element temperature and the element orientation are included as vector displayed in each element.

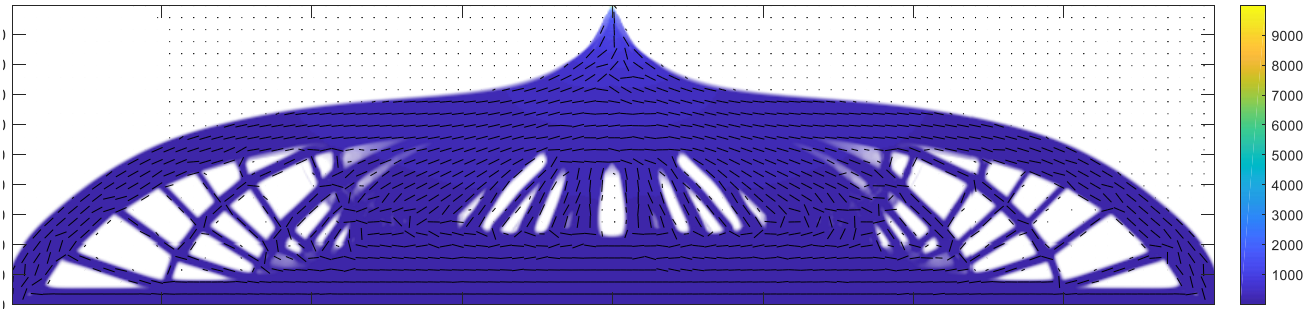

Figure 2: Final Topology for Compliance Optimization Showing Temperature Field

The strain energy-optimized part converges readily to solid or void. In both optimizations, the element orientations converge intuitively as the elements are aligned along the directions of truss-like members.

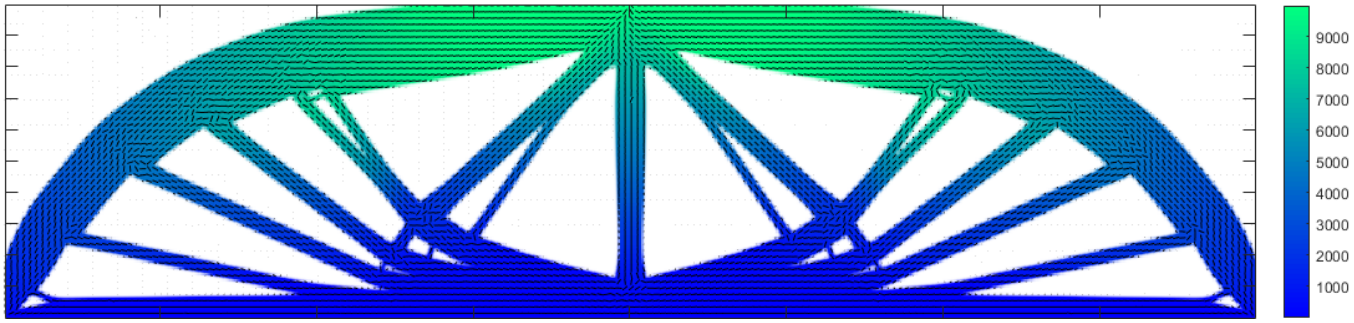

Figure 3: Final Topology for Strain Energy Optimization showing Temperature Field

Conclusions

Stress-Based Performance Comparison

Table 1 shows that the compliance optimization has a lower final compliance value than the strain energy optimization, and the strain energy optimization has a lower strain energy than the compliance optimization, as expected. This is not surprising but does make it difficult to determine which optimization obtained "better" results. Here we consider other performance metrics to assess the 'goodness' of the designs.

Final Performance of Optimized Parts		
	Compliance Optimization	Strain Energy Optimization
Final Compliance (J)	111,610	5,596,800
Final Strain Energy (J)	85,101	29,652

Table 1: Final Performance of Optimized Parts

Although compliance and strain energy are both energy-based design metrics, comparing the stress-based performance of the part can indicate which part is closer to failure. The Von Mises stress is commonly used as a failure criterion for ductile materials and was used in [12] to compare part performance of constant-temperature weakly coupled systems.

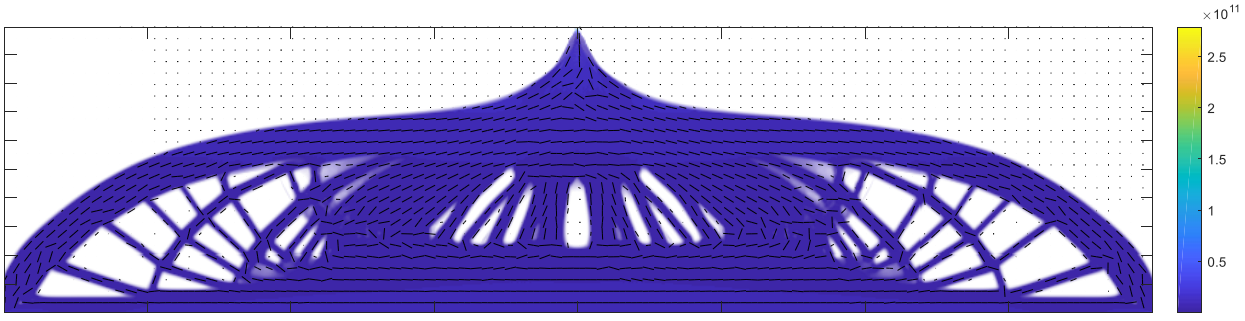

Figure 5: Von Mises Stress Distribution for Compliance-Optimized Structure

The maximum Von Mises stress in the compliance-optimized case is $278.48\ GPa$. It is only obtained at the point where the load is applied, and the remainder of the structure is at a much lower Von Mises stress.

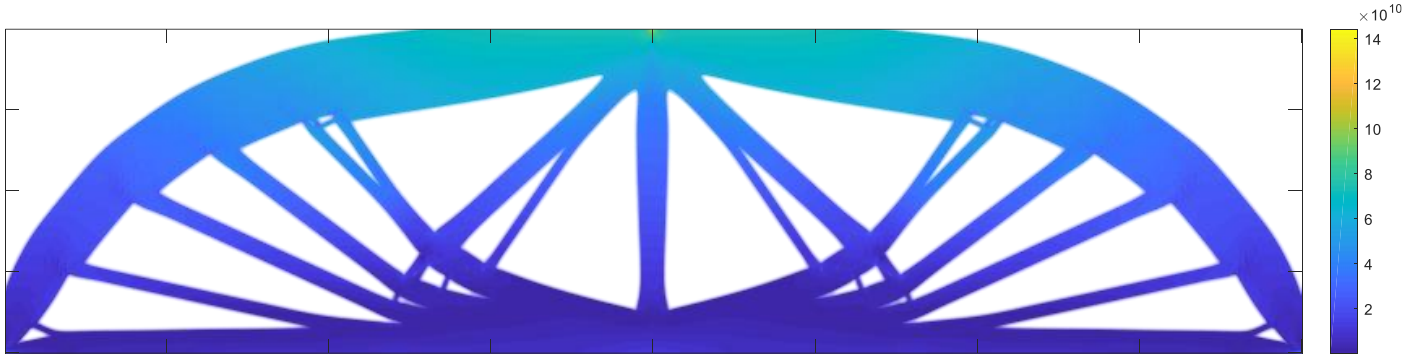

Figure 6: Von Mises Stress Distribution for Strain Energy-Optimizes Structure

The maximum Von Mises stress in the strain energy-optimized case is $143.9\ GPa$. Note that this is lower than the maximum Von Mises stress in the compliance-optimized case, but that a much larger region of the structure experiences stresses near this maximum. Our findings here are similar to the results in [12] for isotropic isothermal weakly coupled systems.

Convergence Concerns

For both strain energy and compliance, it was noted in a parameter study that the relative values of the move limits affect the convergence and final design of the structure, and higher orientation move limits can prevent convergence. This is likely because the orientation optimization method assumes that each element can be considered independently, although each element's orientation affects the response of the overall structure and, therefore, other element orientations. Therefore, we find that the element independent treatment of material angle is only valid for small move limits.

Proof-of-Concept Part Production – Preliminary Results

The final topologies presented here can be produced in standard desktop 3D printers. First, any densities that have not converged are rounded up or down to finalize the design. Then, a series of streamlines are generated in the part, using a streamline generator by Dr. Keith Ma [18]. An in-house Matlab script generates the gcode to print beads along the generated streamlines, and output from this code serves as input for our Makerbot Replicator 2 to print the desired part. The authors intend to replicate this procedure using Baylor's large-area polymer printer to produce larger parts.

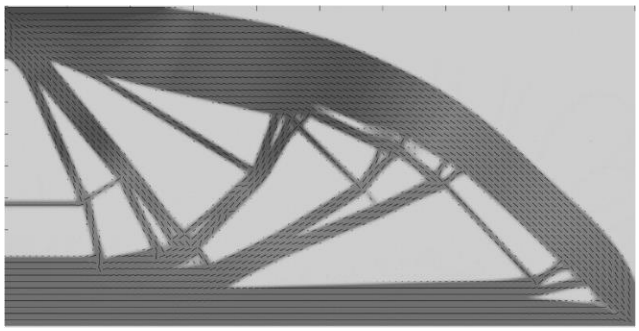

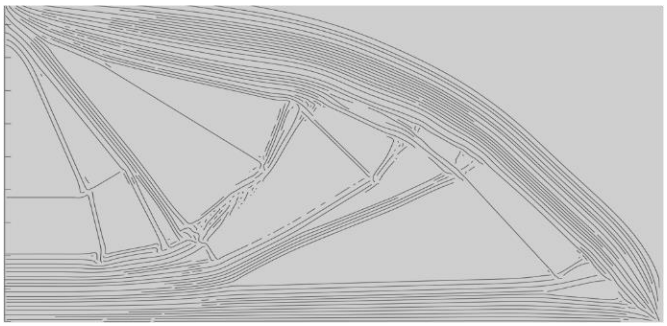

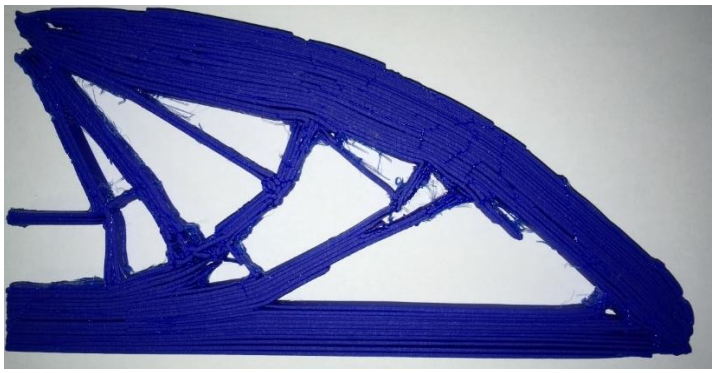

Figure 6: Part Manufacturing Process Showing Final Topology, Streamlines used for Toolpath, and Part

Summary and Next Steps

Summary of Results

The topology optimization algorithm used here was developed to optimize the structure of additively manufactured parts. The anisotropic material properties and thermal stresses similar to those that arise in the polymer printing process were included in the optimization process. The algorithm converges to final part designs for compliance and strain energy minimization, which can be produced in proof-of-concept parts.

A comparison of the final topologies indicates that optimizing strain energy yields parts with $143.9\ GPa$ maximum Von Mises stress, which is lower than the maximum Von Mises stress of $278.5\ GPa$ found in the compliance-optimized part. This is in accordance with the results in [12] and [13], where isotropic optimization was performed under a fixed temperature field.

Future Work

Although the design-dependent temperature field used here is a step forward, it does not fully capture the transient cooling effects in the additive manufacturing process. Modeling the heat transfer as transient instead of steady state will more accurately model the system. One-dimensional modeling of the cooling process has been done at Oak Ridge National Laboratory [19], which provides an overview of the thermal behavior of large-area additive manufacturing systems.

Additionally, the two-dimensional optimization done here demonstrates the effectiveness of the method but applying the method to a three-dimensional design space will yield more useful parts. These parts usually are weakest perpendicular to the build plane, so this extra anisotropy will be considered. Also, the cooling is dependent on the order that the polymer beads are extruded, so optimization over toolpath may need to be included. Printing and testing parts on Baylor's large-area polymer printer will determine if there are additional factors that affect the part performance.

Acknowledgements

The authors wish to thank our colleagues in Baylor's Scientific Innovation in Complex Engineering Materials group for their insights into the additive manufacturing process and polymer behavior. Additional thanks go to Dr. Keith Ma who posted a streamline generation Matlab code online that was used for the generation of test parts.

Bibliography

1. Bendsoe, Martin Philip, Kikuchi, Noboru. “Generating Optimal Topologies in Structural Design Using a Homogenization Method.” Computer Methods in Applied Mechanics and Engineering (1988): 197-224. DOI: 10.1016/0045-7825(88)90086-2
2. Sigmund, O. “A 99 Line Topology Optimization Code Written in Matlab.” Structural and Multidisciplinary Optimization (2001): 120-127. DOI: 10.1007/s001580050176
3. Wang, Michael Yu, Wang, Xiaoming, Guo, Dongming. “A Level Set Method for Structural Topology Optimization.” Computer Methods in Applied Mechanics and Engineering (2003): 227-246. DOI: 10.1016/S0045-7825(02)00559-5
4. Svanberg, Krister. “The Method of Moving Asymptotes – a New Method for Structural Optimization.” International Journal for Numerical Methods in Engineering (1987): 359-373. doi:10.1002/nme.1620240207
5. Bendsoe, M. P., Sigmund, O. Topology Optimization Theory, Methods, and Applications. Germany: Springer-Verlag Berlin Heidelberg 2003
6. Hoglund, Robert. “An Anisotropic Topology Optimization Method For Carbon Fiber-Reinforced Fused Filament Fabrication.” Masters Thesis, Baylor University.
7. Jiang, Dale. “Three Dimensional Topology Optimization with Orthotropic Material Orientation Design for Additive Manufacturing Structures.” Masters Thesis, Baylor University.
8. Jiang, Delin, Hoglund, Robert, Smith, Douglas E. “Continuous Fiber Angle Topology Optimization for Polymer Composite Deposition Additive Manufacturing Applications.” Fibers (2019): DOI: 10.3390/fib7020014
9. Luo, J. H., Gea, H. C. “Optimal Orientation of Orthotropic Materials Using an Energy Based Method.” Structural Optimization (1998): 230-236. DOI: 10.1007/BF01203536
10. Deaton, Joshua. “Design of Thermal Structures Using Topology Optimization.” Dissertation for Doctor of Philosophy, Wright State University 2009.
11. Pederson, Pauli, Pederson, Niels. “Strength Optimized Designs of Thermoelastic Structures.” Structural and Multidisciplinary Optimization (2010): 681-691. DOI: 10.1007/s00158-010-0535-5
12. Zhang, Weihong, Yang, Jungang, Xu, Yingjie, Gao, Tong. “Topology Optimization of Thermoelastic Structures: Mean Compliance Minimization or Elastic Strain Energy Minimization.” Structural and Multidisciplinary Optimization (2014): 417-429. DOI: 10.1007/s00158-013-0991-9
13. Neiford, David John, Grandhi, Ramana V., Deaton, Joshua D., Beran, Philip S. “Level-Set Topology Optimization of Thermoelastic Structures – a Comparison of Compliance, Strain Energy, and Stress Objectives.” 2018 Multidisciplinary Analysis and Optimization Conference. Atlanta, Georgia, June 25-29 2018. AIAA Aviation Forum. DOI: 10 2514/6 2018-3577
14. H. L. Tekinalp, V. Kunc, G. M. Velez-Garcia, C. E. Duty, L. J. Love, A. K. Naskar, C. A. Blue, and S. Ozcan, “Highly oriented carbon fiber–polymer composites via additive manufacturing,” Compos. Sci. Technol., vol. 105, pp. 144–150, Dec. 2014.
15. Dechaumphai, Pramote, Thornton, Earl. “Enhanced Thermal-Structural Analysis by Integrated Finite Elements,” Flight Dynamics Laboratory. 1984.

16. D. A. Tortorelli & P. Michaleris. “Design sensitivity analysis: Overview and review, Inverse Problems in Engineering,” 1:1, 71-105, (1994) DOI: 10.1080/174159794088027573

17. Ramsey, Jackson S., Smith, Douglas E. “Topology Optimization of Coupled Thermomechanical Analysis for Additive Manufacturing.” SAMPE Conference (2019).

18. Ma, Keith. “Evenly Spaced Streamlines,” Mathworks File Exchange, 06-Oct-2016. Accessed on 06-Jun-2019 from https://www.mathworks.com/matlabcentral/fileexchange/59476-evenly-spaced-streamlines

19. Compton, Brett G., Post, Brian K., Duty, Chad E., Love, Lonnie, Kunc, Vlastimil. “Thermal Analysis of Additive Manufacturing of Large-Scale Thermoplastic Polymer Composites.” Additive Manufacturing (2017): 77-86. DOI: 10.1016/j.addma.2017.07.006